[Journal of the Faculty of Science, Hokkaidô University, Japan, Ser. VII, Vol. I, No. 3, 1959]

Transition from Dispersive RAYLEIGH Waves to Sound Waves in a Layer over a Half Space Absolutely Rigid

Kyôzi TAZIME

(Received Sept. 25, 1959)

Abstract

Dispersive RAYLEIGH waves in a layer over a half space absolutely rigid were investigated pretty thoroughly by GIESE[1].

He ignored $\mathbf{M}^{(2)}$-type of the waves, assuming that this type had much smaller amplitude than that of $\mathbf{M}^{(1)}$-type. However the present paper suggests that his assumption had no theoretical foundation.

Moreover he did not refer to any higher order of **M**-waves. Indeed he treated media having POISSON's ratios larger than 0.25, but the character of **M**-waves was obscure at the limit when POISSON's ratio arrived at 0.50.

It is the main purpose of the present paper to clear up the last defect just mentioned.

It must be noted that notations and expressions in this paper will follow those employed and obtained in the previous paper by the present author[2].

1. Superficial waves in a liquid layer

Taking space-coordinates as shown in Fig. 1 and assuming a line source at $z=E$, displacement-potential of superficial waves can be written as

$$[\phi]^{(l)}{}_{=\mathbf{M}_0} = -\frac{2\pi\omega}{\bar{\alpha}^2 H}\left(\frac{1}{U}-\frac{1}{c}\right)\sin\bar{\alpha}E\,\sin\bar{\alpha}z\,, \tag{1.1}$$

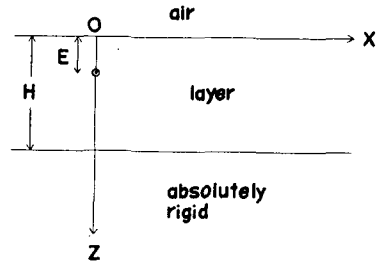

Fig. 1. Space-coordinates under consideration.

being the same expression as that obtained in the case of a plate[3].

In (1.1) the characteristic equation is given by

$$\mathbf{M}^{(l)} = 0 \quad \text{that is} \quad \cos \bar{\alpha} H = 0 \tag{1.2}$$

or

$$\bar{\alpha} H = (2l+1)\pi/2, \ (l = 0, 1, 2, \ldots) . \tag{1.3}$$

2. Dispersive RAYLEIGH waves in a solid layer

In a solid layer, as well known, $\mathbf{M}^{(1)}$ and $\mathbf{M}^{(2)}$-waves must exist. The displacement-potential of them can be expressed, by means of a method similar to that used in a solid plate, as follows.

(i) $c \geqq v_p > v_s$; $\alpha = \bar{\alpha}$, $\beta = \bar{\beta}$.

$$\left.\begin{aligned}
[\phi]_{\mathbf{M}=0} = &-\frac{\pi\omega}{\bar{\alpha}^2 H}\left(\frac{1}{U}-\frac{1}{c}\right)\Big[\cos\bar{\alpha}(z-E)\left\{(1-AA')\sin\bar{\alpha}H\cos\bar{\beta}H\right.\\
&\left.+(1+AA')\cos\bar{\alpha}H\sin\bar{\beta}H\right\}+\sin\bar{\alpha}(z+E)\left\{-(A-A')\cos\bar{\alpha}H\cos\bar{\beta}H\right.\\
&\left.+(A+A')\sin\bar{\alpha}H\sin\bar{\beta}H\right\}+\cos\bar{\alpha}(z+E)\left\{(A-A')\sin\bar{\alpha}H\cos\bar{\beta}H\right.\\
&\left.+(A+A')\cos\bar{\alpha}H\sin\bar{\beta}H\right\}\Big]/N,\\
[\psi]_{\mathbf{M}=0} = &\ i\frac{\pi\omega}{\bar{\alpha}^2 H}\left(\frac{1}{U}-\frac{1}{c}\right)\Big[B\left\{(1+A')\cos\bar{\alpha}(E-H)\cos\bar{\beta}(z-H)\right.\\
&\left.-(1-A')\sin\bar{\alpha}(E-H)\sin\bar{\beta}(z-H)\right\}+B'\left\{(1+A)\cos\bar{\alpha}E\cos\bar{\beta}z\right.\\
&\left.-(1-A)\sin\bar{\alpha}E\sin\bar{\beta}z\right\}\Big]/N,\\
N = &\left\{(1-AA')+(\bar{\beta}/\bar{\alpha})(1+AA')\right\}\sin\bar{\alpha}H\cos\bar{\beta}H+\left\{(1+AA')\right.\\
&\left.+(\bar{\beta}/\bar{\alpha})(1-AA')\right\}\cos\bar{\alpha}H\sin\bar{\beta}H,
\end{aligned}\right\} \tag{2.1}$$

in which the characteristic equation is given by

$$\mathbf{M} = 0 \text{ that is } \sin^2\tfrac{1}{2}(\bar{\alpha}+\bar{\beta})H - AA'\sin^2\tfrac{1}{2}(\bar{\alpha}-\bar{\beta})H = \tfrac{1}{2}(1-AA'-BC') . \tag{2.2}$$

A' in (2.1) and (2.2) means PP-reflecting coefficient as to displacement -potential on the lower boundary in a superficial layer.

Letting rigidity of the layer tend to zero, A must approach to -1 and B to zero, as already mentioned in the case of a plate. On the other hand, A' will approach to 1 at the same time, whichever value phase-velocity may have, as illustrated in Fig. 2. B' as well as C' will approach to zero again, being $B'^2 = (\bar{\alpha}/\bar{\beta})(1-A'^2)$. In this case, $[\psi]_{\mathbf{M}=0}$ in (2.1) must be zero and (2.2) will be reduced to

$$\left\{(\tan\bar{\alpha}H/2-1)(\tan\bar{\beta}H/2+1)\right\}\left\{(\tan\bar{\alpha}H/2+1)(\tan\bar{\beta}H/2-1)\right\} = 0 , \tag{2.3}$$

that is

$$\bar{\alpha}H = (2l+1)\pi/2 \quad \text{or} \quad \bar{\beta}H = (2m+1)\pi/2 , \tag{2.4}$$

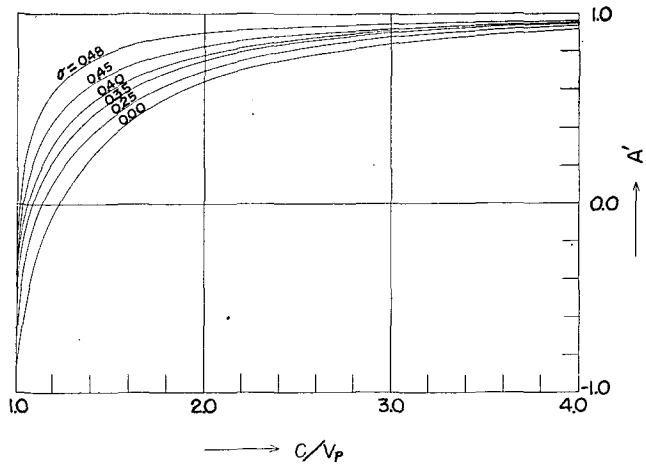

Fig. 2. PP-reflecting coefficient on the lower boundary in a layer.

where l and m represent positive integers, indicating orders of these curves. The former of (2.4) coincide with (1.3) and one sees that $[\phi]_{M=0}$ in (2.1) will coincide with that in (1.1).

On the other hand, when the latter of (2.4) is satisfied, $[\psi]_{M=0}$ in (2.1) must be zero.

Thus letting rigidity of the layer tend to zero, branches corresponding to $(\tan \bar{\alpha}H/2-1)(\tan \bar{\alpha}H/2+1)=0$ alone can survive, otherwise amplitudes of displacement-potentials become zero. The surviving two branches coincide respectively with the branches of the even and odd orders of superficial waves in a liquid layer.

(ii) $v_p \geqq c \geqq v_s$; $\alpha=-i\hat{\alpha}$, $\beta=\bar{\beta}$.

$$\left.\begin{aligned}
[\phi]_{M=0} &= \frac{\pi\omega}{\hat{\alpha}^2 H}\left(\frac{1}{U}-\frac{1}{c}\right)\Big[\cosh\hat{\alpha}(z-E)\left\{e^{\hat{\alpha}H}\sin(\bar{\beta}H-\delta-\delta)\right.\\
&\quad \left.+e^{-\hat{\alpha}H}\sin(\bar{\beta}H+\delta+\delta)\right\}-\left\{e^{\hat{\alpha}(z+E-H)}\sin(\bar{\beta}H-\delta-\delta)\right.\\
&\quad \left.+e^{-\hat{\alpha}(z+E-H)}\sin(\bar{\beta}H+\delta-\delta')\right\}\Big]/N,\\
[\psi]_{M=0} &= i\frac{\pi\omega}{\hat{\alpha}^2 H}\left(\frac{1}{U}-\frac{1}{c}\right)\left(\frac{2\hat{\alpha}}{\bar{\beta}}\right)\Big[(\sin 2\delta)^{1/2}\left\{e^{\hat{\alpha}(E-H)}\sin(\bar{\beta}(z-H)-\delta)\right.\\
&\quad \left.-e^{-\hat{\alpha}(E-H)}\sin(\bar{\beta}(z-H)+\delta')\right\}+(\sin 2\delta')^{1/2}\left\{e^{\hat{\alpha}E}\sin(\bar{\beta}z-\delta)\right.\\
&\quad \left.-e^{-\hat{\alpha}E}\sin(\bar{\beta}z+\delta)\right\}\Big]/N,\\
N &= e^{\hat{\alpha}H}\sin(\bar{\beta}H-\delta-\delta')+e^{-\hat{\alpha}H}\sin(\bar{\beta}H+\delta+\delta')\\
&\quad +(\bar{\beta}/\hat{\alpha})\left\{e^{\hat{\alpha}H}\cos(\bar{\beta}H-\delta-\delta')-e^{-\hat{\alpha}H}\cos(\bar{\beta}H+\delta+\delta')\right\},
\end{aligned}\right\}\quad(2.5)$$

in which the characteristic equation is given by

$\mathbf{M}=0$ that is

$$\left\{e^{\alpha H/2}\cos\tfrac{1}{2}(\bar{\beta}H-\delta-\delta')-e^{-\alpha H/2}\cos\tfrac{1}{2}(\bar{\beta}H+\delta+\delta')\right\}$$
$$\cdot\left\{e^{\alpha H/2}\sin\tfrac{1}{2}(\bar{\beta}H-\delta-\delta\ )+e^{-\alpha H/2}\sin\tfrac{1}{2}(\bar{\beta}H+\delta+\delta')\right\}$$
$$=\sin(\delta+\delta')\pm\left\{\sin^2(\delta+\delta')-\sin^2(\delta-\delta')\right\}^{1/2}. \tag{2.6}$$

δ' in (2.5) and (2.6) means phase-lag of displacement-potential at PP -reflection on the lower boundary of the layer. Letting rigidity of the layer tend to zero, δ must approach to zero, as already mentioned in the case of a plate. On the other hand, δ' will approach to $\pi/2$ for all values of phase -velocity between v_p and v_s as illustrated in Fig. 3. In this case, $[\psi]_{\mathbf{M}=0}$ in (2.5) must be zero and (2.6) will be reduced to

$$\cosh\alpha H\cdot\cos\bar{\beta}H=0. \tag{2.7}$$

Because $\cosh\alpha H$ cannot be zero, $\cos\bar{\beta}H$ must always be zero. Owing to

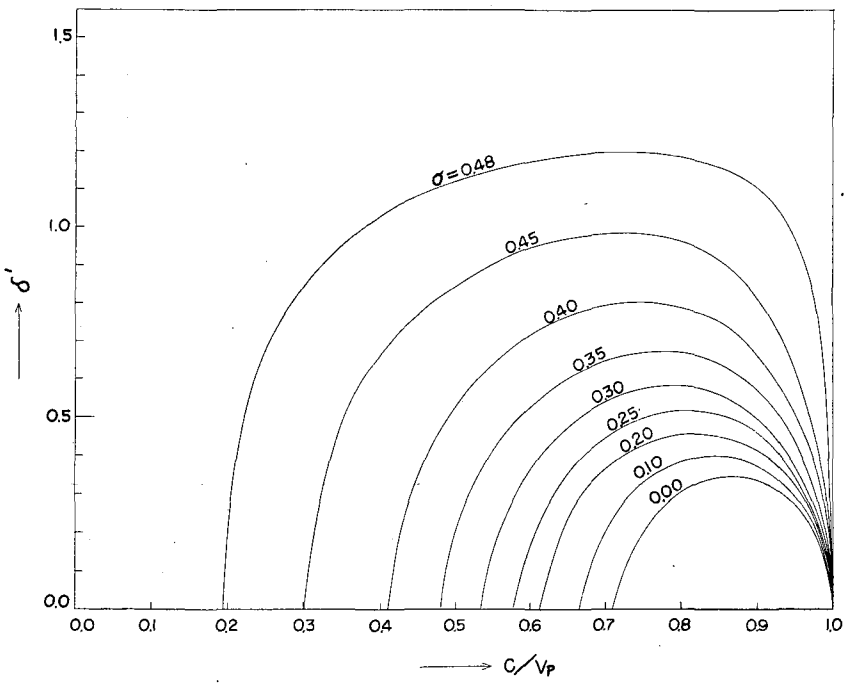

Fig. 3. Phase-lag at PP-reflection on the lower boundary.

this result, one sees that $[\phi]_{M=0}$ in (2.5) also becomes zero. No wave, therefore, can survive in the present case.

(iii) $v_p > v_s \geqq c$; $\alpha = -i\hat{\alpha}$, $\beta = -i\hat{\beta}$.

$$\left.\begin{aligned}
[\phi]_{M=0} = & -i\frac{\pi\omega}{\hat{\alpha}^2 H}\left(\frac{1}{U}-\frac{1}{c}\right)\Big[\cosh\hat{\alpha}(z-E)\{(1-AA')\sinh\hat{\alpha}H\cosh\hat{\beta}H \\
& +(1+AA')\cosh\hat{\alpha}H\sinh\hat{\beta}H\} - \sinh\hat{\alpha}(z+E) \\
& \cdot\{(A-A')\cosh\hat{\alpha}H\cosh\hat{\beta}H+(A+A')\sinh\hat{\alpha}H\sinh\hat{\beta}H\} \\
& +\cosh\hat{\alpha}(z+E)\{(A-A')\sinh\hat{\alpha}H\cosh\hat{\beta}H \\
& +(A+A')\cosh\hat{\alpha}H\sinh\hat{\beta}H\}\Big]/N, \\
[\psi]_{M=0} = & -i\frac{\pi\omega}{\hat{\alpha}^2 H}\left(\frac{1}{U}-\frac{1}{c}\right)\Big[B\{(1+A)\cosh\hat{\alpha}(E-H)\cosh\hat{\beta}(z-H) \\
& +(1-A')\sinh\hat{\alpha}(E-H)\sinh\hat{\beta}(z-H)\}+B'\{(1+A)\cosh\hat{\alpha}E \\
& \cdot\cosh\hat{\beta}z+(1-A)\sinh\hat{\alpha}E\sinh\hat{\beta}z\}\Big]/N, \\
N = & -i\Big[\{(1-AA')+(\hat{\beta}/\hat{\alpha})(1+AA')\}\sinh\hat{\alpha}H\cosh\hat{\beta}H \\
& +\{(1+AA')+(\hat{\beta}/\hat{\alpha})(1-AA')\cosh\hat{\alpha}H\sinh\hat{\beta}H,
\end{aligned}\right\} \quad (2.8)$$

in which the characteristic equation is given by

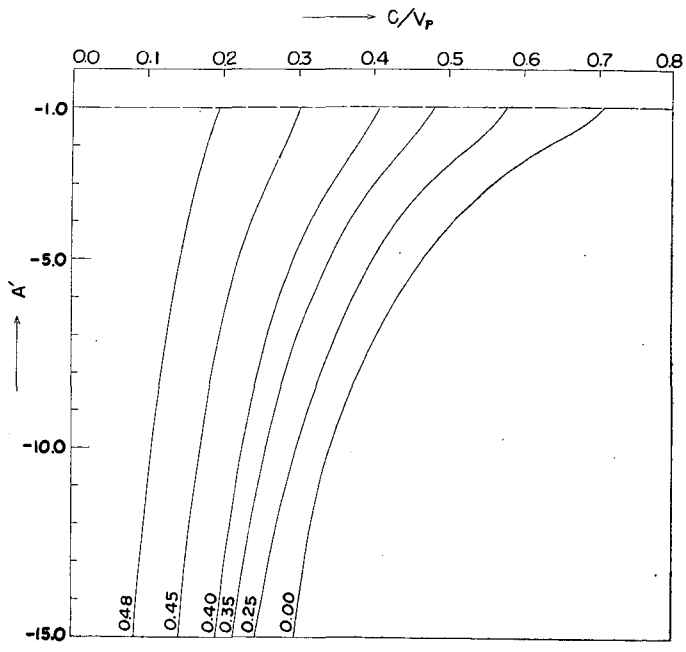

Fig. 4. PP-reflecting coefficient on the lower boundary.

$\mathbf{M}=0$ that is

$$\sinh^2 \tfrac{1}{2}(\hat{\alpha}+\hat{\beta})H - AA' \sinh^2 \tfrac{1}{2}(\hat{\alpha}-\hat{\beta})H = \tfrac{1}{2}(BC'+AA'-1) = l^2 . \qquad (2.9)$$

A' in (2.8) and (2.9) means again PP-reflecting coefficient on the lower boundary of the layer.

Letting rigidity of the layer tend to zero, A must be confined to -1, as already mentioned in the case of a plate. On the other hand, A' is to be confined also to -1, as illustrated in Fig. 4. Because B and B' are again zero in this case, $[\psi]_{\mathrm{M}=0}$ in (2.8) must be zero and (2.9) will be reduced to

$$\cosh(\hat{\alpha}H/2)\sinh(\hat{\beta}H/2)\sinh(\hat{\alpha}H/2)\cosh(\hat{\beta}H/2) = 0 . \qquad (2.10)$$

As $\cosh(\hat{\alpha}H/2)\sinh(\hat{\alpha}H/2)\cosh(\hat{\beta}H/2)$ cannot be zero, $\sinh(\hat{\beta}H/2)$ must be zero, with the result that $[\phi]_{M=0}$ in (2.8) is also zero.

It has been recognized in this section that dispersive RAYLEIGH waves in a solid layer should be reduced to superficial waves in a liquid layer at the limit when rigidity is taken as zero. In the following section, processes of transition will be investigated.

3. Numerical calculations of the dispersion-curves for various POISSON's ratios

At the limit when POISSON's ratio arrives at 0.50, A' in Fig. 2 must coincide with 1 and A with -1 for any value of c/v_p.

Turning attention to A' and A for general POISSON's ratio, one sees that A' will always approach again to 1 and A to -1 if $c/v_p \gg 1$.

Considering the above two circumstances with Fig. 2, it may be expected that the nearer σ approaches to 0.50, the wider becomes the range satisfying (2.3).

If $c/v_p=1$, one sees $A'=A=-1$ for any value of σ, with the result that the right hand side of (2.2) becomes zero, because $BC'=0$ in this case. Namely one has

$$\sin \bar{\alpha}H \sin \bar{\beta}H = 0 ,$$

being the same as the relation in the case of a plate.

If $c/v_s=1$, one sees again $A'=A=-1$ for any value of σ. Thus one has

$$\sinh \hat{\alpha}H \sin \bar{\beta}H = 0 .$$

Because $\sinh \hat{\alpha}H$ cannot be zero in this case, dispersion-curves must always approach to $\sin \bar{\beta}H=0$ near $c=v_s$.

As one has seen by now, for any value of σ,

$$\cos \bar{\alpha} H = 0 \quad \text{and} \quad \cos \bar{\beta} H = 0 \tag{3.1}$$

might be the bases with respect to dispersion-curves of RAYLEIGH waves in a layer resting on a half space absolutely rigid, if $c/v_p > 1$. On the other hand,

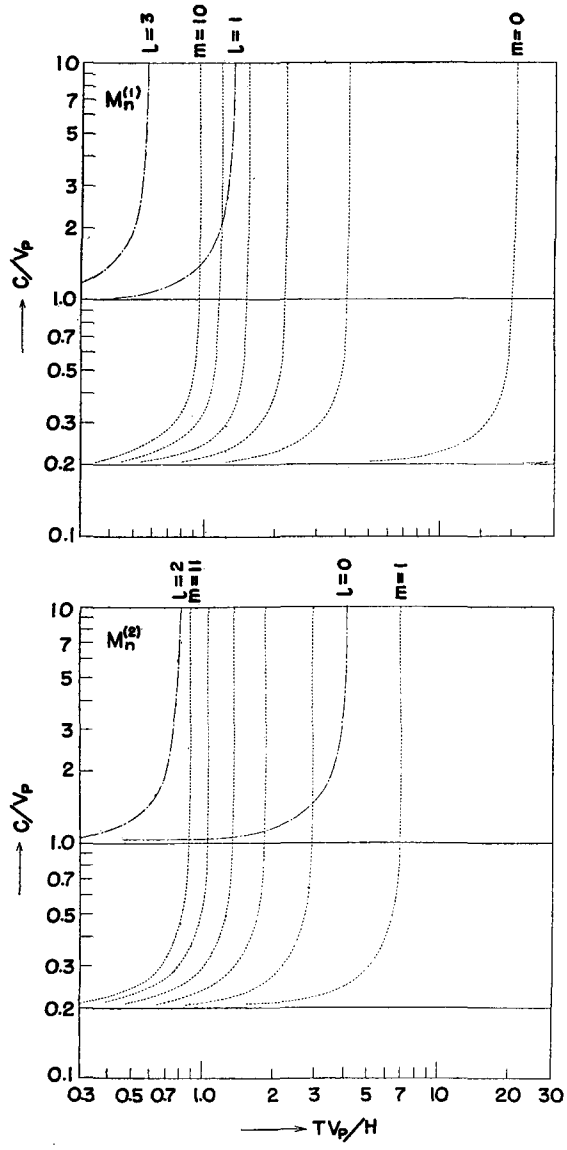

Fig. 5. Chain-lines correspond to $\bar{\alpha}H = (2l+1)\pi/2$, while dotted lines to $\bar{\beta}H = (2m+1)\pi/2$. $\sigma = 0.48$.

$$\sin \bar{\beta} H = 0 \tag{3.2}$$

might be the base near $c = v_s$.

In Fig. 5 are shown the curves given by (3.1), that is (2.4). Classification of $\mathbf{M}^{(1)}$ and $\mathbf{M}^{(2)}$ in Fig. 5 follows that in the case of a plate. Odd l and even m belong to $\mathbf{M}^{(1)}$, on the contrary even l and odd m to $\mathbf{M}^{(2)}$. The curves given by $\cos \bar{\beta} H = 0$ must be shifted to the rightward with increase in σ, though the curves given by $\cos \bar{\alpha} H = 0$ need not. In Fig. 5, for an example, the curves for $\sigma = 0.48$ are exhibited.

(i) Now $l^2 = \frac{1}{2}(1 - AA' - BC')$ in (2.2) has been calculated at first and is illustrated in Fig. 6. If $c/v_p \gg 1$, one sees that l is equal to unity for any value of σ and (2.2) may be resolved into the next two branches:

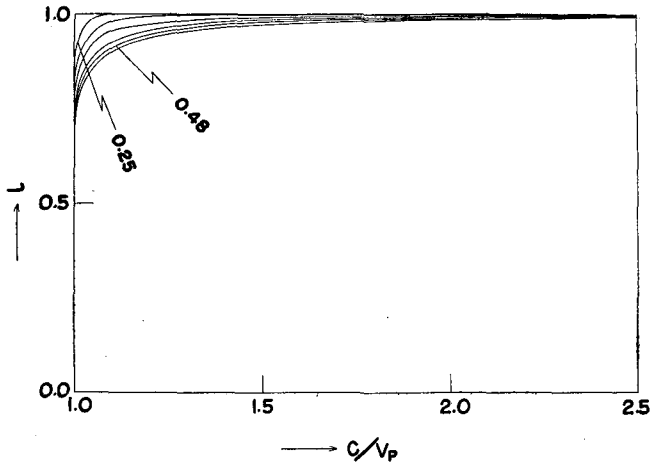

Fig. 6. The relation between l in (2.2) and c/v_p.

$$\left.\begin{aligned} &\cos\left(\frac{\bar{\beta}}{\xi} + \frac{\bar{\alpha}}{\xi}\right)\frac{\xi H}{2} + (-AA')^{1/2} \sin\left(\frac{\bar{\beta}}{\xi} - \frac{\bar{\alpha}}{\xi}\right)\frac{\xi H}{2} = 0 \quad \text{for } \mathbf{M}^{(1)}, \\ &\cos\left(\frac{\bar{\beta}}{\xi} + \frac{\bar{\alpha}}{\xi}\right)\frac{\xi H}{2} - (-AA')^{1/2} \sin\left(\frac{\bar{\beta}}{\xi} - \frac{\bar{\alpha}}{\xi}\right)\frac{\xi H}{2} = 0 \quad \text{for } \mathbf{M}^{(2)}, \end{aligned}\right\} \tag{3.3}$$

where classification of $\mathbf{M}^{(1)}$ and $\mathbf{M}^{(2)}$ depends on the limit when (3.3) will coincide with (2.3) in which $A = -1$ and $A' = 1$. It will be very easy, as in the case of a plate, to obtain dispersion-curves from (3.3).

If c/v_p approaches to 1, l differs from unity and (2.2) cannot be resolved into factors. The process of graphical solution for this case, or

$$\sin\left(\frac{\bar{\beta}}{\xi} + \frac{\bar{\alpha}}{\xi}\right)\frac{\xi H}{2} = \pm \left\{l^2 + AA' \sin^2\left(\frac{\bar{\beta}}{\xi} - \frac{\bar{\alpha}}{\xi}\right)\frac{\xi H}{2}\right\}^{1/2} \tag{3.4}$$

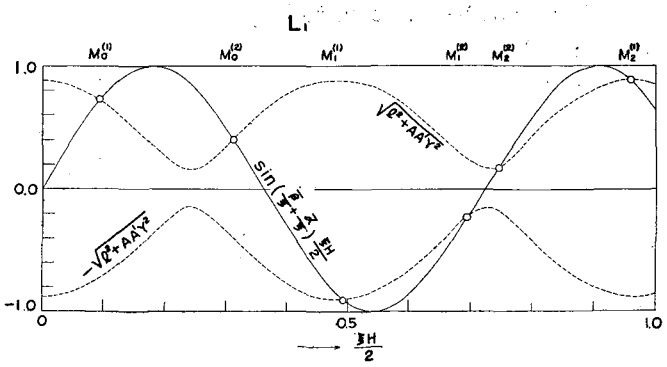

Fig. 7. An example of graphical solutions for (2.2).
$\sigma=0.48$ and $c/v_p=1.5$.

is shown by Fig. 7. Owing to intersection of $\cos \bar{\alpha}H=0$ with $\cos \bar{\beta}H=0$, systematic classification of $\mathbf{M}^{(1)}$ and $\mathbf{M}^{(2)}$ is somewhat disturbed, if c/v_p is not much larger than unity. This disturbance appears in Fig. 7 between $\mathbf{M}_1^{(2)}$ and $\mathbf{M}_2^{(2)}$.

(ii) (2.6) may be rewritten by

$$\sin(\bar{\beta}H-\delta-\delta') = e^{-2\bar{\alpha}H}\sin(\bar{\beta}H+\delta+\delta') \pm 2\,e^{-\bar{\alpha}H}(\sin 2\delta \sin 2\delta')^{1/2} \quad \text{for } c/v_s \gtrless \sqrt{2}\,. \tag{3.5}$$

An example of graphical solution for (3.5) is exhibited in Fig. 8 where $\mathbf{M}_n^{(1)}$ and $\mathbf{M}_n^{(2)}$ appear in turn regularly, because $\cos \bar{\alpha}H=0$ does not exist in the present region and no disturbance can occur.

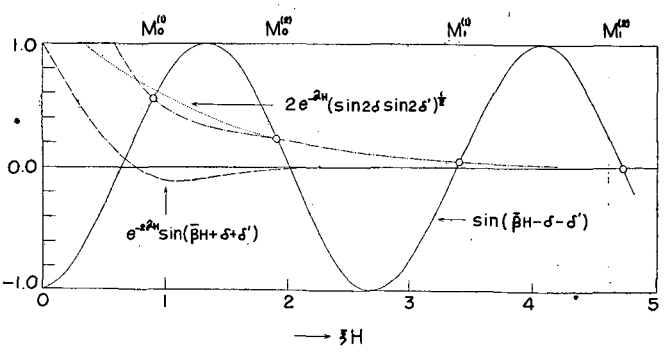

Fig. 8. An example of graphical solution for (3.5).
$\sigma=0.48$ and $c/v_p=0.50$.

If $c/v_p>1$, it cannot be expected to be possible to classify the branch by Fig. 7 alone. In order to avoid this difficulty, Fig. 5 and Fig. 8 must be compared with Fig. 7.

(iii) (2.9) may be rewritten by

$$\sinh\left(\frac{\hat{\alpha}}{\xi}+\frac{\hat{\beta}}{\xi}\right)\frac{\xi H}{2}=\left\{l^2+AA'\sinh^2\left(\frac{\hat{\alpha}}{\xi}-\frac{\hat{\beta}}{\xi}\right)\frac{\xi H}{2}\right\}^{1/2} \tag{3.6}$$

from which $\mathbf{M}_0^{(1)}$ alone will be obtained.

If c becomes smaller than v_s, A and A' will decrease to become remarkably smaller than -1 at once and l^2 in (2.9) will coincide with AA'. In this case (3.6) will be reduced to

$$\sinh\left(\frac{\hat{\alpha}}{\xi}+\frac{\hat{\beta}}{\xi}\right)\frac{\xi H}{2}=l\cosh\left(\frac{\hat{\alpha}}{\xi}-\frac{\hat{\beta}}{\xi}\right)\frac{\xi H}{2}. \tag{3.7}$$

As l in (2.9) is illustrated in Fig. 9, graphical solution of (3.7) is very easy.

Thus the dispersion-curves for $\sigma=0.48$ have been obtained, as shown by full lines in Fig. 10 where the other lines correspond respectively to those in

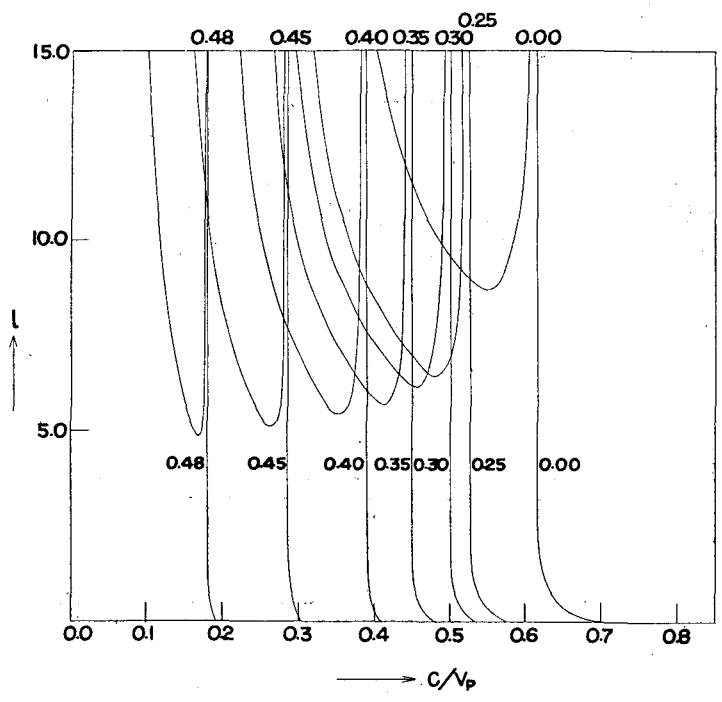

Fig. 9. l in (2.9).

Fig. 5. Dispersion-curves for the other POISSON's ratios are also shown in Figs. 11 to 14 in the same manner as those in Fig. 10.

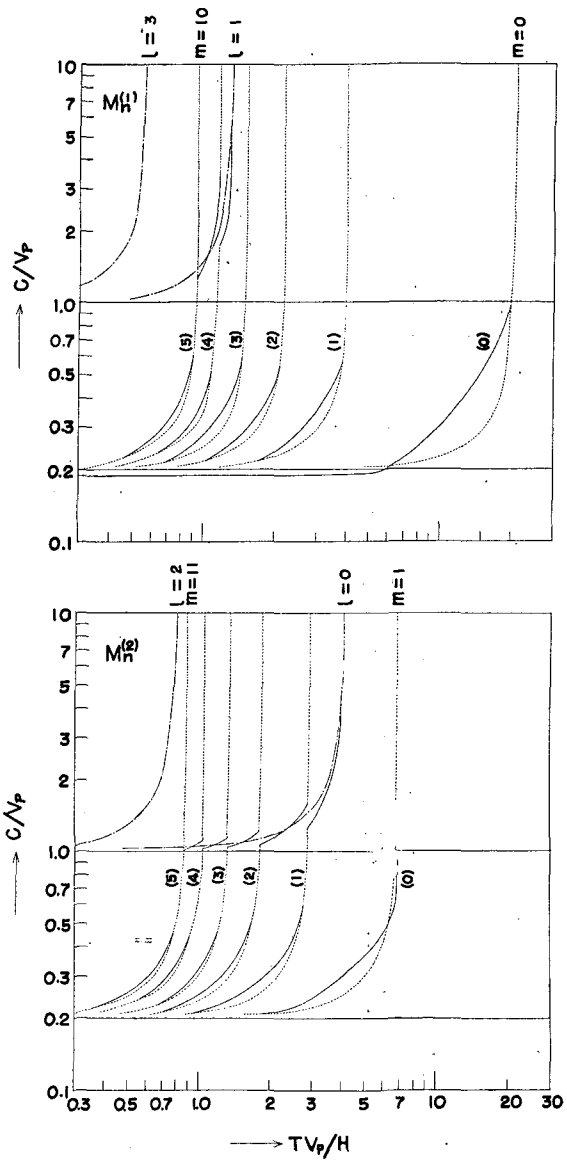

Fig. 10. Dispersion-curves for $\sigma = 0.48$.

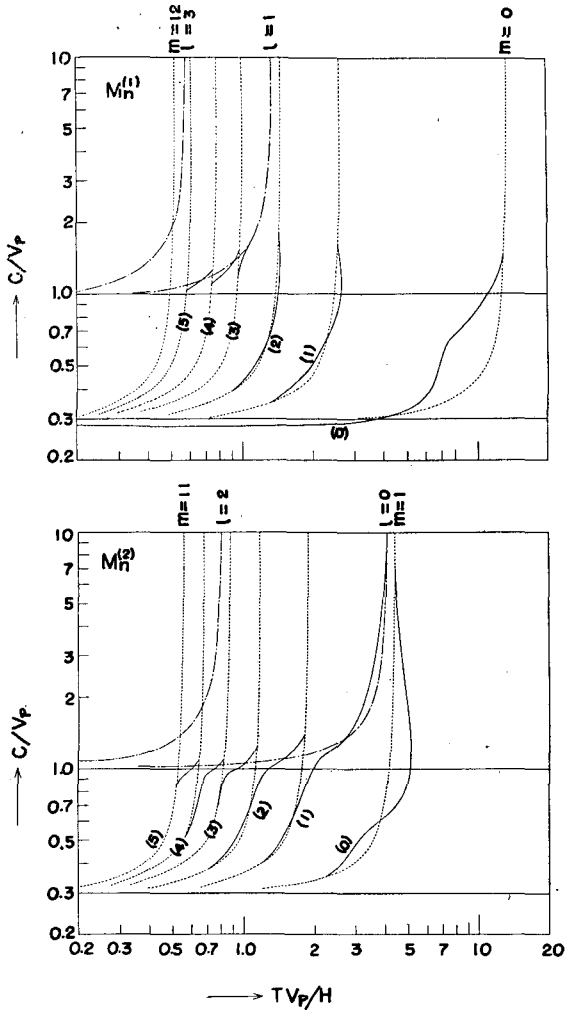

Fig. 11. Dispersion-curves for $\sigma=0.45$.

4. Conclusions

(1) If $c/v_p \gg 1$, the dispersion-curves always coincide with any one of the curves given by (2.4), whatever value σ may have.

(2) If $c/v_p \gg 1$, periods of the former and of the latter equation in (2.4) should coincide with each other under the next condition,

$$2m+1=(2l+1)(v_p/v_s)\,. \tag{4.1}$$

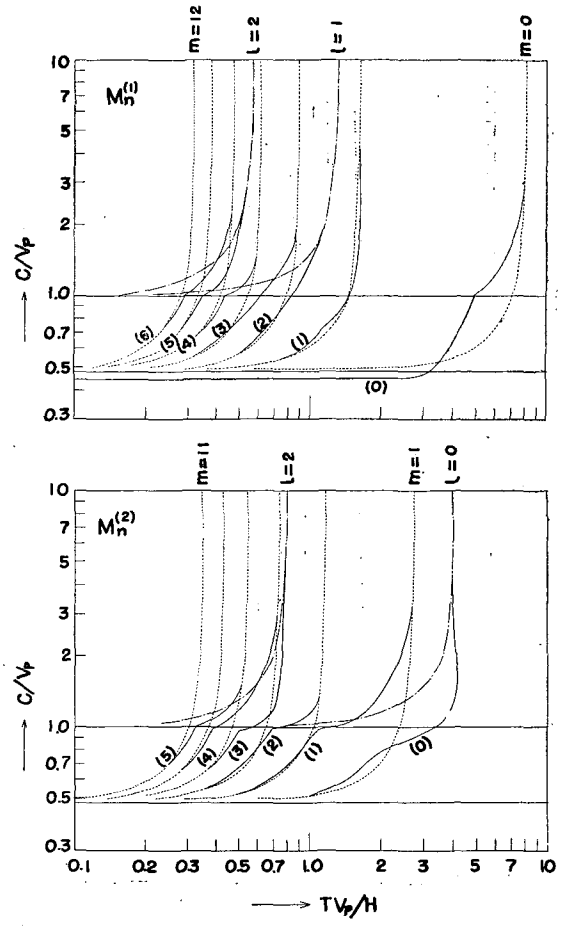

Fig. 12. Dispersion-curves for $\sigma=0.35$.

Because odd orders of m must correspond to even orders of l, the lowest order of m satisfying (4.1) is 1 for $l=0$, resulting in $v_p/v_s=3.0$ or $\sigma=0.44$.

If $\sigma<0.44$, no curve indicated by m exists to the right of the curve indicated by $l=0$ with which $\mathbf{M}_0^{(2)}$ always coincides in this case.

If $\sigma>0.44$, on the other hand, some curves indicated by m appear to the right of $l=0$. The nearer σ approaches to 0.50, the larger becomes the number of m-curves to the right of $l=0$.

(3) On dotted lines in Fig. 10 to 14 amplitudes of displacement-potentials are zero, though the dispersion-curves may be calculated.

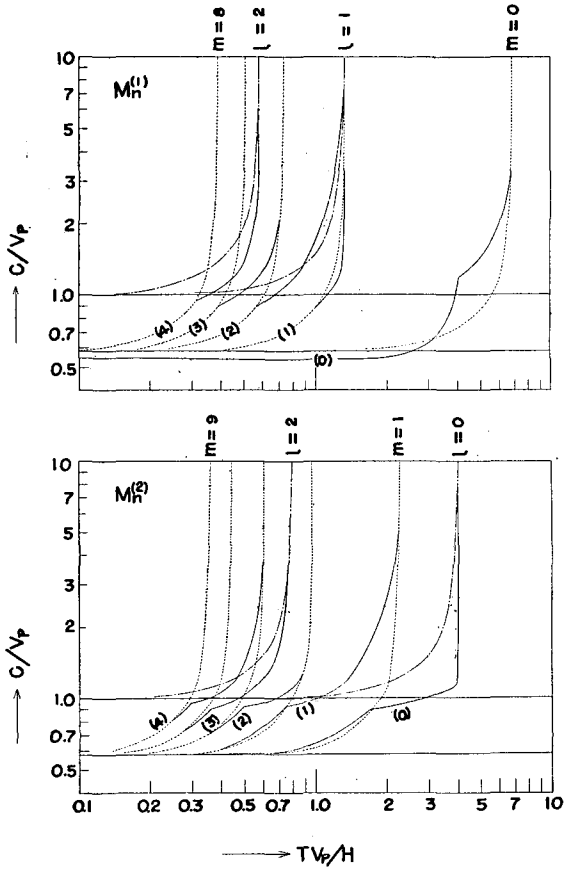

Fig. 13. Dispersion-curves for $\sigma=0.25$.

(4) It may be expected, on the other hand, that on chain-lines amplitudes will be large. Indeed amplitudes on full lines differ from zero, but the maximum amplitude must be attained on chain-lines at

$$Tv_p/H = 4/(2l+1)\,. \tag{4.2}$$

(5) It has been found to be wrong, if $\sigma>0.44$ for $\mathbf{M}_n^{(2)}$ and if $\sigma>0.22$ for $\mathbf{M}_n^{(1)}$, to say that the lower the order of dispersive RAYLEIGH waves is, the larger may become the amplitude of the wave. This situation is completely different from the case of LOVE waves and of sound waves, consisting respectively of either S or P-waves alone.

(6) (4.2) means "quarter wave-length law". It was a wonder that such

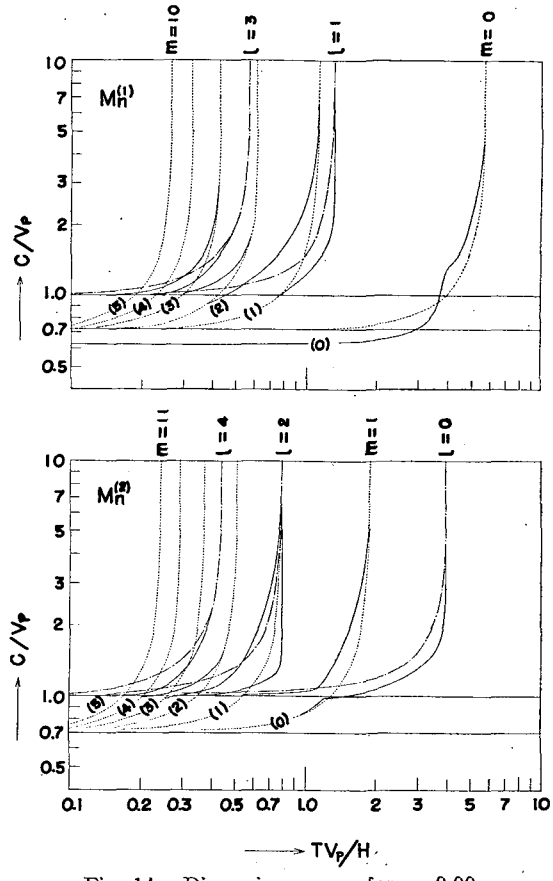

Fig. 14. Dispersion-curves for $\sigma=0.00$.

a law as (4.2) had been often experienced[4] for dispersive RAYLEIGH waves in field-experiments, in spite of the existence of P-wave as well as of S-wave in the layer. But it has been understood in the present paper that among many branches of dispersive RAYLEIGH waves a few of them must correspond to $\cos \bar{\alpha}H=0$ and others to $\cos \bar{\beta}H=0$. Amplitudes of the latter ones cannot be so large that the law containing v_p alone will become important. It must be also noticed that the order of dispersive RAYLEIGH waves cannot be determined from the observed "wave-length law".

(7) Picking out $\mathbf{M}_0^{(1)}$, $\mathbf{M}_0^{(2)}$ and the curve for $l=0$ alone from Figs. 10 to 14, one will obtain Fig. 15. In this figure $\mathbf{M}_0^{(1)}$ and $\mathbf{M}_0^{(2)}$ diverge from the curve for $l=0$ when σ approaches to 0.50. Thus it should not be expected

that two curves, for solid and for liquid waves, will coincide with each other at the limit of $\sigma=0.50$. The process of transition from solid to liquid cannot be understood by Fig. 15.

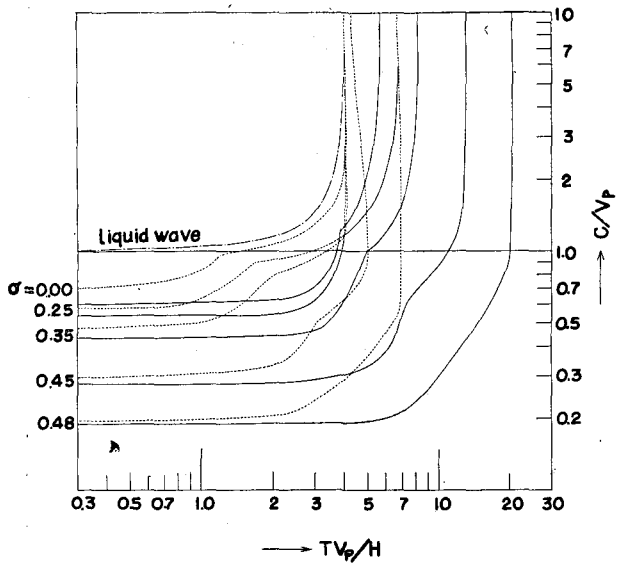

Fig. 15. Comparison of dispersion-curves for the zeroth order of M-waves to the curve for the zeroth order of liquid waves.

According to the present investigation, one sees, the process is very complicated. When σ approaches to 0.50, the zeroth order of liquid waves is constructed approximately of many higher orders $\mathbf{M}_n^{(2)}$-waves and the first order of liquid waves is approximately constructed of many higher orders of $\mathbf{M}_n^{(1)}$-waves and so on.

5. Remarks

If attention is confined in the region of $Tv_p/H \ll 1$ and $c/v_p \approx 1$ in Fig. 5, a similar lattice to MINDLIN's[5] may be formed. The dispersion-curve in this region takes also "terrace-like structure" named by MINDLIN in the case of a plate.

Acknowledgment. The author expresses his thanks to Mr. Toshihiro HIGASHIYAMA, Mr. Makoto KISHI and Miss Miyako MUROTA for their helps in numerical calculations. The author wishes again to express his thanks to Ministry of Education for a grant from the Science Research Fund 1958 by the aid of which the present investigation was facilitated.

References

1) GIESE, Peter: Die Bestimmung der elastischen Eigenschaften und der Mächtigkeit von Lockerböden mit Hilfe von speziellen Rayleigh-Wellen. Gerl. Beitr. Geophys., **66** (1957), 274–312.
2) TAZIME, Kyozi: Ray-theoretical Construction of Dispersive Rayleigh Waves. Journ. Phys. Earth, **6** (1958), 81–89.
3) TAZIME, Kyozi: Transition from Solid to Liquid Superficial Waves in a Plate. Journ. Phys. Earth, **6** (1958), 91–99.
4) TAZIME, Kyozi: Wave Groups Generated by a Very Small Explosion. Journ. Phys. Earth, **4** (1956), 113–126.
TAZIME, Kyozi: Relations between Charge Amounts and Periods in Resulting Seismic Wave Groups. Journ. Phys. Earth, **5** (1957), 51–59.
5) TOLSTOY, Ivan: Resonant Frequencies and High Modes in Layered Wave Guides. J. Acoust. Soc. Am., **28** (1956), 1182–1192.
TOLSTOY, Ivan and USDIN, Eugene: Wave Propagation in Elastic Plates. J. Acoust. Soc. Am., **29** (1957), 37–42.